

Ab initio prediction of giant magnetostriction and spin-reorientation in strained Au/FeCo/MgO heterostructure

P.V. Ong, Nicholas Kioussis



PII: S0304-8853(15)30372-3
DOI: <http://dx.doi.org/10.1016/j.jmmm.2015.07.065>
Reference: MAGMA60430

To appear in: *Journal of Magnetism and Magnetic Materials*

Received date: 20 June 2015
Revised date: 18 July 2015
Accepted date: 22 July 2015

Cite this article as: P.V. Ong and Nicholas Kioussis, *Ab initio* prediction of giant magnetostriction and spin-reorientation in strained Au/FeCo/MgO heterostructure, *Journal of Magnetism and Magnetic Materials* <http://dx.doi.org/10.1016/j.jmmm.2015.07.065>

This is a PDF file of an unedited manuscript that has been accepted for publication. As a service to our customers we are providing this early version of the manuscript. The manuscript will undergo copyediting, typesetting, and review of the resulting galley proof before it is published in its final citable form. Please note that during the production process errors may be discovered which could affect the content, and all legal disclaimers that apply to the journal pertain.

P. V. Ong* and Nicholas Kioussis†

Department of Physics and Astronomy, California State University Northridge, Northridge, California 91330, USA

(Dated: July 22, 2015)

Employing *ab initio* electronic structure calculations we have investigated the magnetostrictive properties and the effect of epitaxial strain on the magnetic anisotropy (MA) of Au/FeCo/MgO heterostructure. Under small expansive strain on the FeCo layer the system exhibits an in-plane MA. The calculations reveal that the strain dependence of the MA is nonlinear and that the FeCo film undergoes a spin reorientation at a critical strain between 2 to 4%. The underlying mechanism is the strain-induced shift of the spin-orbit coupled *d*-states of the Fe atoms. We predict a giant magnetostriction coefficient of about 420×10^{-6} in the heterostructure.

PACS numbers: PACS numbers: 75.30.Gw, 75.70.Cn, 75.85.+t, 73.20.-r

I. INTRODUCTION

Magnetic nano-junctions of heavy-metal/ferromagnet/insulator (HM/FM/I) are of great interest in spintronic devices such as high density and nonvolatile magnetic random access memory (MRAM). The magnetization reversal is induced by spin-polarized current via the spin transfer torque (STT-RAM)¹ or by an electric field via the magnetoelectric effect (MeRAM).²⁻⁴ Au/FeCo/MgO is a promising system since recent experiments by Shiota *et al.* showed voltage-induced switching of the magnetic easy axis from in- to out-of-plane direction.²

Since there is often a fairly large lattice mismatch (4-5%) between the I, the FM and HM layers, the component layers are under large uniaxial strain which can in turn modify significantly the magnetic properties of the heterostructure including the magnetic anisotropy (MA) which arises from the spin orbit coupling (SOC). *Ab initio* calculations have recently investigated the effect of hydrostatic pressure on the MA of bulk FeCo alloys.^{5,6}

In this work we report results of *ab initio* electronic structure calculations of the effect of epitaxial strain on the MA of the Au/FeCo/MgO (001) heterostructure. We find that the strain dependence of MA is nonlinear and that the system undergoes a spin reorientation transition at a critical strain between 2 to 4%. The underlying mechanism is the strain-induced shift of spin-orbit coupled *d*-states of the interfacial Fe ions. We also predict that the strain dependence of the MA yields a giant magnetostriction coefficient of 420 ppm (parts per million).

II. COMPUTATIONAL METHOD AND MODEL

First-principles density functional calculations were performed within the framework of the plane wave projector augmented wave formalism,⁷ as implemented in the Vienna *ab initio* simulation package (VASP) code.⁸⁻¹⁰ The generalized gradient approximation¹¹ has been employed to treat the exchange-correlation

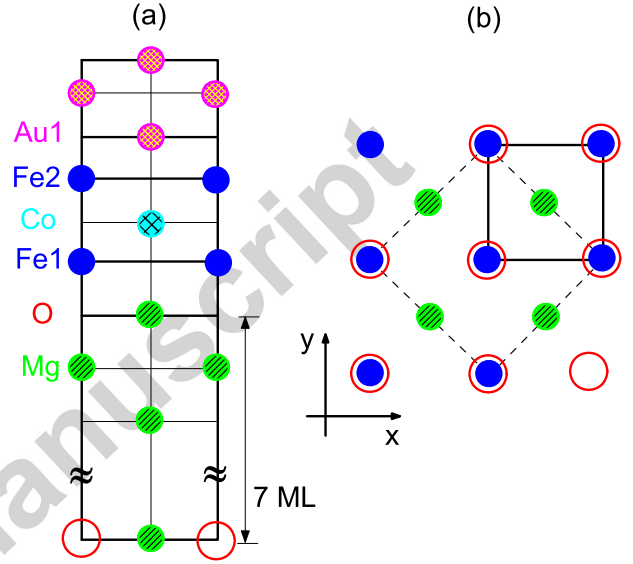


FIG. 1. (Color online) (a) Side view of the Au/FeCo/MgO (001) heterostructure consisting of three monolayers (MLs) of fcc Au on top of three MLs of B2-type FeCo on top of seven MLs of rock-salt MgO; (b) Top view of atomic configuration of the FeCo/MgO interface, where the O atoms are atop of Fe atoms.

functional. To simulate the epitaxial growth of the Au/FeCo/MgO junction, we employed a slab supercell along the [001] direction consisting of three monolayers (MLs) of Au, three MLs of B2-type FeCo, seven MLs of rock-salt MgO and a 15Å-thick vacuum region separating the periodic slabs [Fig. 1(a)]. The FeCo/MgO interface is modeled by placing the O atoms atop the Fe atoms [Fig. 1(b)]. The interfacial Fe atoms at the Fe/MgO and Fe/Ta interfaces are denoted by Fe1 and Fe2 atoms, respectively.

We build up supercells by aligning the $\langle 110 \rangle$ axis of MgO and Au with the $\langle 100 \rangle$ axis of FeCo. The FeCo layer is under large expansive strain, η_{FeCo} , of about 4% assuming that the MgO substrate is unstrained. On the other hand, recent experiments showed that ultra-

TABLE I. Calculated interlayer distances (d_{\perp}), spin moment (m_s), orbital moment differences (Δm_o), and MA as a function of strain, η_{FeCo} , on the FeCo. Here, $\Delta m_o \equiv m_o^{[001]} - m_o^{[100]}$, where $m_o^{[001]}$ and $m_o^{[100]}$ are the atomic orbital moments with magnetization oriented along the [001] and [100] directions, respectively.

Strain(%)	d_{\perp} (Å)						$m_s(\mu_B)$			$\Delta m_o(10^{-2}\mu_B)$			MA(erg/cm ²)
	Au3-Au2	Au2-Au1	Au1-Fe2	Fe2-Co	Co-Fe1	Fe1-MgO	Fe1	Fe2	Au1	Fe1	Fe2	Au1	
0	2.191	2.236	1.880	1.501	1.315	2.194	2.656	2.795	0.046	2.1	0.7	-0.6	-0.56
2	2.123	2.169	1.818	1.462	1.272	2.161	2.680	2.808	0.048	1.6	0.2	-0.8	-0.74
4	2.056	2.105	1.757	1.346	1.232	2.130	2.682	2.773	0.048	3.2	-0.5	-0.8	0.32

thin (~ 2 nm) MgO film is significantly compressed to match the lattice constant of the FM film¹². In order to study the effect of lateral strain under different growth conditions, we have varied η_{FeCo} from zero to 4%. At each strain, the magnetic, electronic degrees of freedom and atomic z positions are fully optimized until the atomic forces become less than 5×10^{-3} eV/Å and the change in the total energy between two ionic relaxation steps is smaller than 10^{-6} eV. The plane-wave cutoff energy is 500 eV and the Monkhorst-Pack k -mesh for the relaxation calculations was $15 \times 15 \times 1$. The dipole correction to the total energy is applied.¹³ The valence electrons are treated in the scalar relativistic approximation and the SOC of the valence electrons is included using the second-variation method¹⁴ employing the scalar-relativistic eigenfunctions of the valence states. Employing a $31 \times 31 \times 1$ k -point mesh, the MA per unit interfacial area, A , is determined from $MA = [E_{[100]} - E_{[001]}]/A$, where $E_{[100]}$ and $E_{[001]}$ are the total energies with magnetization along the [100] and [001] directions, respectively.

III. RESULTS AND DISCUSSION

The interlayer atomic distances, spin moment and orbital-moment difference of Fe1, Fe2, and Au1, and MA of the system under various strains on the FeCo are listed in Table I. At $\eta_{FeCo} = 0$, the interlayer distances in the Au cap are larger than those in the FeCo layer. This is due to the large compressive strain on the Au layer, since the lattice constant of bulk Au is larger than that of the B2-type FeCo. In the FM layer, the interlayer Co-Fe1 distance is significantly smaller than that of Fe2-Co due to the displacement of the Co atom. As expected, these distances decrease with increasing expansive strain. The magnitude of spin moments of Fe1 and Fe2 are comparable and vary by less than 1% with strain. Au ions have negligible spin moment, even for the Au1 next to the FM layer. On the other hand, the orbital moment difference $\Delta m_o \equiv m_o^{[001]} - m_o^{[100]}$ of Fe1 is at least 3 times as large as that of Fe2 and exhibits strong strain dependence. Interestingly, a magnetic switching from in-plane to out-of-plane direction occurs with increasing strain in the range from 2% to 4%. Note that the strain variation of MA is nonlinear and correlates to the change of Δm_o

of Fe1.

In order to understand the role of the MgO and the Au cap on the MA we have carried out calculations of the MA of the free standing 3 ML FeCo film (vacuum/FeCo/vacuum) and the MgO/FeCo/vacuum for $\eta_{FeCo} = 0, 4\%$. Under zero strain the MA of the free standing and MgO/FeCo/vacuum systems are 1.28 and 2.70 erg/cm², respectively, indicating an out-of-plane magnetization orientation in sharp contrast to the Au/FeCo/MgO heterostructure which favors in-plane magnetization. At 4% the MA of the free standing and MgO/FeCo/vacuum systems are -0.31 and -0.68 erg/cm², respectively, indicating that both systems undergo a transition from out-of-plane to in-plane direction with increasing strain. These results show that the MgO/FeCo interface provides a large contribution to the perpendicular MA at zero strain which arises from the Fe 3d - O 2p hybridization. It is also interesting to note that the MA of the MgO/FeCo/vacuum system is more sensitive to strain compared to that of the free standing FeCo film. This is due to the sensitivity of the Fe-O bond length and hence the hybridization to strain. The opposite sign of MA for the Au/FeCo/MgO system compared to the corresponding uncapped systems under the same strain is clearly induced by the Au capping layer. The underlying mechanism is the shift in the energy levels of Fe d -states and the changes in energy- and k -resolved distribution of the Fe d -orbital characters, which are induced by the capping layer.

To elucidate the mechanism of the strain effect, we show in Fig. 2 the evolution of the minority-spin Fe1 d -derived bands close to the Fermi energy along a segment of the $\bar{\Gamma} - \bar{M}$ (Σ) direction with increasing strain $\eta_{FeCo} = 0, 2, 4\%$. Within second-order perturbation of the total energy due to SOC constant, ξ , the MA is determined by the matrix elements of the orbital angular momentum operators \hat{L}_x and \hat{L}_z between occupied and unoccupied d -states and by the energy difference between these states. Since the Fe-derived majority spin states are well below the Fermi energy, the MA contribution from the SOC between states of opposite spin can be neglected. Thus, the MA can be expressed as¹⁵

$$MA \propto \xi^2 \sum_{o,u} \frac{|\langle \Psi_o^\downarrow | \hat{L}_z | \Psi_u^\downarrow \rangle|^2 - |\langle \Psi_o^\downarrow | \hat{L}_x | \Psi_u^\downarrow \rangle|^2}{E_u^\downarrow - E_o^\downarrow}, \quad (1)$$

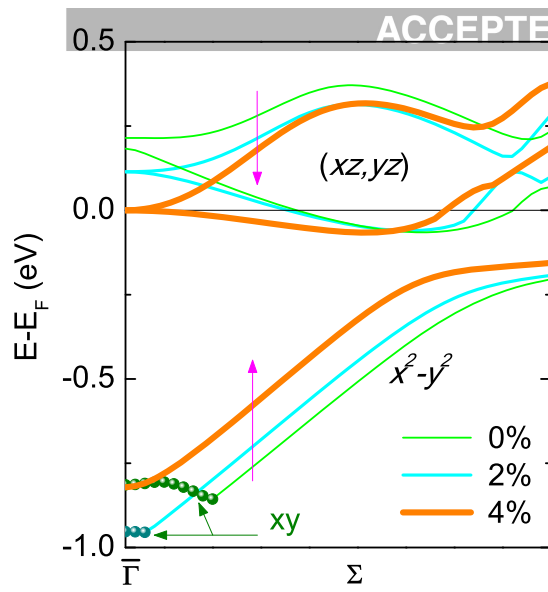


FIG. 2. (Color online) Evolution of the minority-spin Fe1 d -derived bands close to the Fermi energy along a segment of the $\bar{\Gamma} - \bar{M}$ (Σ) direction with increasing strain $\eta_{FeCo}=0, 2, 4\%$. The unoccupied or partially occupied bands around the Fermi level have Fe1 $d_{xz,yz}$ character while the fully occupied bands have Fe1 $d_{x^2-y^2}$ character. For zero and 2% strain, these bands near $\bar{\Gamma}$ (denoted with circles) are of Fe1 d_{xy} character.

where Ψ_o^\uparrow (E_o^\uparrow), and Ψ_u^\downarrow (E_u^\downarrow) are occupied and unoccupied minority-spin states (energies); and $\hat{L}_{x(z)}$ is the x (z) component of orbital angular momentum operator.

At zero strain, the Fe1 $d_{xz,yz}$ -derived states are mainly unoccupied and couple through \hat{L}_x to the occupied Fe1 $d_{x^2-y^2}$ - (green curves below the Fermi level) and d_{xy} -derived states (green circles near $\bar{\Gamma}$) yielding negative MA. At 2% strain, the occupied d_{xy} -derived states around $\bar{\Gamma}$ shift downward (blue circles), leading to an increase in the energy separation to the unoccupied $d_{xz,yz}$. This induces a slight increase in MA at 2%. With further increase of strain to 4%, the $d_{xz,yz}$ band near $\bar{\Gamma}$ becomes occupied resulting to a strong coupling of the pair of occupied and unoccupied $d_{xz,yz}$ states near $\bar{\Gamma}$ through \hat{L}_z . Consequently, the MA increases and the magnetic switching occurs.

We next calculate the magnetoelastic properties of the Au/FeCo/MgO heterostructure. Under distortion, the change of the energy density of the lattice can be expressed to second order in strain as¹⁶:

$$\frac{E(e_i)}{V} = \frac{E_0}{V} - P(V) \frac{\Delta V}{V} + \frac{1}{2} \sum_{i=1}^6 \sum_{j=1}^6 C_{ij} e_i e_j \quad (2)$$

where e_i and C_{ij} is the strain tensor and elastic constants (in Voigt notation), E_0 and V is the energy and volume of the undistorted lattice, $P(V)$ the pressure of the lattice

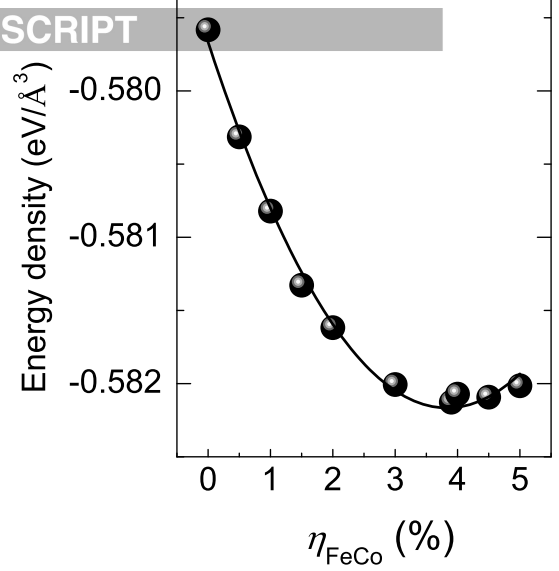


FIG. 3. (Color online) *Ab initio* calculated energy density (solid circles) as a function of strain on FeCo. The solid curve denotes the fit of the points to Eq. (6).

at volume V , and ΔV is the change of the volume due to strain. For cubic lattices, the number of independent elastic constants, C_{ij} , is reduced to three: C_{11} , C_{12} , and C_{44} . For a thin film grown epitaxially along the [001] crystallographic direction, there is no shear strain, *i.e.*, $e_5 = e_6 = 0$ and $e_1 = e_2 = \eta_{FeCo}$ which is in-plane strain on FeCo. The perpendicular strain e_3 is given by¹⁷:

$$e_3 \approx -\frac{2\nu}{1-\nu} \eta_{FeCo} \quad (3)$$

where the Poisson's ratio ν is given by

$$\nu = \frac{C_{12}}{C_{11} + C_{12}} \quad (4)$$

For transition metals, $\nu \approx 1/3$ ^{17,18}, resulting in $C_{12} = \frac{C_{11}}{2}$ and $e_3 \approx -\eta_{FeCo}$. The change in volume $\frac{\Delta V}{V}$ can be calculated to second order in strain as:

$$\frac{\Delta V}{V} = 2e_1 + e_3 + 2e_1 e_3 + e_1^2 = \eta_{FeCo} - \eta_{FeCo}^2. \quad (5)$$

Thus, Eq.(2) can be rewritten in the form

$$\frac{E(e_i)}{V} = \frac{E_0}{V} - P(V) \eta_{FeCo} + [P(V) + C_{11}] \eta_{FeCo}^2. \quad (6)$$

Fig. 3 shows the *ab initio* calculated energy density of Au/FeCo/MgO as a function of η_{FeCo} . By fitting the data to the Eq. (6), we find that $P(V)=20.8$ GPa and $C_{11}=251.8$ GPa. For the bulk $Fe_{50}Co_{50}$ system, the experimental value of C_{11} is 244 GPa (inferred from $C' = (C_{11} - C_{12})/2=61$ GPa)¹⁹.

The strain dependence of the *ab initio* calculated MA

$$MA = K_2^i + B_1^2 t \frac{2C_{11} + D_{11}}{(C_{11} + D_{11})^2} + B_1 t \left[1 + \frac{C_{11}^2}{(C_{11} + D_{11})^2} \right] \eta_{FeCo} + \frac{D_{11} t}{2} \left[1 - \frac{C_{11}^2}{(C_{11} + D_{11})^2} \right] \eta_{FeCo}^2. \quad (7)$$

Here, K_2^i is the effective interface magnetocrystalline anisotropy, t is the FM thin film thickness, and B_1 and D_{11} are the first and second order magnetoelastic coefficients, respectively. Using the calculated $C_{11}=251.8$ GPa, the FM film thickness $t=2.677$ Å, we find that $B_1=-8.0 \times 10^8$ erg/cm³, $D_{11}=44.8 \times 10^{10}$ erg/cm³, and $K_2^i=-0.61$ erg/cm², respectively. For comparison, for bulk Fe₅₀Co₅₀, the experimental value of the first-order magnetoelastic coefficient is $B_1^v=-3 \times 10^8$ erg/cm³.¹⁹

The magnetostriction coefficient can be determined from²¹

$$\lambda_{001} = -\frac{2B_1}{3(C_{11} - C_{12})} \quad (8)$$

Using the calculated values above for B_{11} , C_{11} , and $C_{12} = C_{11}/2$, we find that $\lambda_{001} = 424 \times 10^{-6}$. This value is one third of that estimated for the Fe₃₄Co₆₆ thin film ($\lambda_{001} = 1,300 \times 10^{-6}$) under the assumption of vanishing λ_{111} ,²² and is of the same order of magnitude as the giant values reported for Tb-based thin films.²³

In summary, we have presented *ab initio* electronic structure calculations that investigate the effect of epitaxial strain on the MA of the Au/FeCo/MgO epitaxial heterostructure. At zero strain on the FM layer the junction exhibits in-plane MA due to the large $\langle x^2 - y^2 | \hat{L}_x | (xz, yz) \rangle$ and $\langle xy | \hat{L}_x | (xz, yz) \rangle$ spin-orbit coupling of the Fe atom at the FeCo/MgO interface. The strain dependence of MA is nonlinear. We predict magnetic switching of the magnetic easy axis from in- to out-of-plane orientation at a critical strain between 2 to 4%. The underlying mechanism lies on the strain-induced shift of the spin-orbit coupled *d*-states of the interfacial Fe atom. We predict a giant magnetostriction coefficient of 424 ppm in the heterostructure. These results demonstrate that strain engineering can open an avenue to tailor the magnetic properties for spintronic applications.

ACKNOWLEDGMENTS

This research was supported by NSF Grant No. ERC-Translational Applications of Nanoscale Multiferroic Systems (TANMS)-1160504.

* phuongvu.ong@csun.edu

† nick.kioussis@csun.edu

¹ C. Chappert, A. Fert, F. N. Van Dau, Nat. Mater. **6**, 813 (2007).

² Y. Shiota, T. Maruyama, T. Nozaki, T. Shinjo, M. Shiraishi, and Y. Suzuki, Appl. Phys. Express **2**, 063001 (2009).

³ T. Maruyama, Y. Shiota, T. Nozaki, K. Ohta, N. Toda, M. Mizuguchi, A. A. Tulapurkar, T. Shinjo, M. Shiraishi, S. Mizukami, Y. Ando, and Y. Suzuki, Nature Nanotech. **4**, 158 (2009).

⁴ W.-G. Wang, M. Li, S. Hageman, and C. L. Chien, Nature Mater. **11**, 64 (2012).

⁵ S. Pascarelli, M. P. Ruffoni, A. Trapananti, O. Mathon, G. Aquilanti, S. Ostanin, J. B. Staunton, and R. F. Pettifer, Phys. Rev. Lett. **99**, 237204 (2007).

⁶ T. Burkert, L. Nordström, O. Eriksson, and Olle Heinonen, Phys. Rev. Lett. **93** 027203 (2004).

⁷ P. E. Blöchl, Phys. Rev. B **50**, 17953 (1994).

⁸ G. Kresse and J. Furthmüller, Phys. Rev. B **54**, 11169 (1996).

⁹ G. Kresse and J. Furthmüller, Comput. Mater. Sci. **6**, 15 (1996).

¹⁰ G. Kresse and J. Hafner, Phys. Rev. B **48**, 13115 (1993).

¹¹ J. P. Perdew, in *Electronic Structure of Solids*, edited by P. Ziesche and H. Eschrig (Akademie Verlag, Berlin, 1991),

p. 11.

¹² S. Yuasa, T. Nagahama, A. Fukushima, Y. Suzuki, and K. Ando, Nature Mater. **3**, **868** (2004).

¹³ J. Neugebauer and M. Scheffler, Phys. Rev. B **46**, 16067 (1992).

¹⁴ D. D. Koelling and B. N. Harmon, J. Phys C: Solid State Phys. **10**, 3107 (1977).
Phys. Rev. B **89**, 094422 (2014).

¹⁵ D.-S Wang, R. Wu, A. J. Freeman, Phys. Rev. B **47**, 14932 (1993).

¹⁶ M. J. Mehl, B. M. Klein, and D. A. Papaconstantopoulos, in *Intermetallic Compounds: Principles and Applications*, edited by J. H. Westbrook and R. L. Fleischer (John Wiley & Sons Ltd., London, 1994).

¹⁷ D. Sander, Rep. Prog. Phys. **62**, 809 (1999).

¹⁸ H. M Ledbetter and R. P. Reed, J. Phys. Chem. Ref. Data **2**, 531 (1973).

¹⁹ A. E. Clark, J. B. Restorff, M. WunFogle, D. Wu, and T. A. Lograsso, J. Appl. Phys. **103**, 07B310 (2008).

²⁰ Derivation of this magnetoelastic equation and complete MA data for fitting are to be published elsewhere.

²¹ P. Bruno *Physical origins and theoretical models of magnetic anisotropy* (Ferienkurse des Forschungszentrums Jülich, Jülich, 1993).

²² D. Hunter, W. Osborn, K. Wang, N. Kazantseva, J. Hattrick-Simpers, R. Suchoski, R. Takahashi, M. Young,

Accepted manuscript